Chinese Chemical Letters 37 (2026) 111121

Contents lists available at ScienceDirect

Chinese Chemical Letters

journal homepage: www.elsevier.com/locate/cclet

Unprecedented diphenyl ether hybrids and spiro-diphenyl ether with antioxidant activity from *Aspergillus* sp. F1-8A associated with toad venom

Hai-Ying Yu[a], Yu-Wei Huang[a], Li-Ping Lin[a,*], Ren-Xiang Tan[a,b]

[a] State Key Laboratory of Technologies for Chinese Medicine Pharmaceutical Process Control and Intelligent Manufacture, School of Pharmacy, Nanjing University of Chinese Medicine, Nanjing 210023, China
[b] State Key Laboratory of Pharmaceutical Biotechnology, Institute of Functional Biomolecules, School of Life Sciences, Nanjing University, Nanjing 210033, China

ARTICLE INFO

Article history:
Received 27 December 2024
Revised 14 March 2025
Accepted 19 March 2025
Available online 25 March 2025

Keywords:
Diphenyl ether hybrids
Spiro-diphenyl ethers
γ-Butyrolactone
Cyclopentenone
Aspergillus
Bufo gargarizans Cantor
Antioxidant activity

ABSTRACT

Asplactones A–E (**1**–**5**), five unique diphenyl ether hybrids, along with two rare spiro-diphenyl ethers, aspviolaceols A (**6**) and B (**7**), were isolated and characterized from *Aspergillus* sp. F1–8A, an endophytic fungus associated with the parotoid glands of *Bufo gargarizans* Cantor. Compounds **1**–**5** represent the first examples of diphenyl ether hybrids fused with unusual moieties, including conjugated γ-butyrolactone and cyclopentenone. Compounds **6** and **7** are the first known natural spiro-diphenyl ethers, with **6** featuring an uncommon 6/6/6/6-membered carbon skeleton, and **7** possessing a distinct 6/6/6/6/6/6-membered diphenyl ether spiro-heterodimer carbon framework. Structural elucidation was performed using a combination of spectroscopic techniques, X-ray crystallography, and quantum-chemical calculations, and plausible biosynthetic pathways were proposed. Biologically, compounds **1**, **2**, **4**, **6**, and **7** exhibited antioxidant activity comparable to or surpassing that of vitamin C in 1,1-diphenyl-2-picrylhydrazyl (DPPH) and 2,2′-azino-bis(3-ethylbenzothiazoline-6-sulfonate) (ABTS), and ferric reducing power assays. They also significantly improved cell viability in H_2O_2-induced oxidative injury assays using A549 cells.

© 2025 Published by Elsevier B.V. on behalf of Chinese Chemical Society and Institute of Materia Medica, Chinese Academy of Medical Sciences.

Diphenyl ethers (DPEs) are well-documented in microorganisms and plants, exhibiting a wide range of bioactive properties, including antibacterial, antioxidant, antitumor, antihemolytic, neuroprotective, and anti-Alzheimer effects [1–3]. Among these, gerfelin, a notable diphenyl ether, has been identified as a novel inhibitor of geranylgeranyl diphosphate synthase, isolated from *Beauveria felina* QN22047 [4]. Similarly, γ-butyrolactone, a five-membered heterocycle with ester functionality, has garnered significant attention in drug discovery due to its presence in numerous biologically active molecules [5]. Several Food and Drug Administration (FDA)-approved drugs containing γ-butyrolactone serve diverse purposes, including as diuretics, anticancer agents, contraceptives, and treatments for heart disease and glaucoma [6]. The conjugated cyclopentenone (CP) moiety, another important pharmacophore, plays a pivotal role in anticancer agents such as cyclopentenone prostaglandins (CyPGs) and clavulones [7,8]. Despite the growing discoveries of both natural and synthetic DPEs [3,9], γ-butyrolactones [10], and CP derivatives [11], hybrids of DPEs fused with conjugated γ-butyrolactones and CPs, as well as spiro-DPEs, remain undescribed.

Aspergillus is a genus of ubiquitous fungi with both significant pathological and therapeutic importance [12,13]. Recent studies have identified 361 new secondary metabolites from *Aspergillus* species between 1915 and 2020 [14]. The search for novel bioactive structures in endophytic fungi has become a major research focus, with *Aspergillus* serving as a valuable reservoir of bioactive secondary metabolites [15,16]. These species produce a wide range of metabolites, including polyketides, alkaloids, terpenoids, and sterols, with over half exhibiting notable bioactivities [17,18]. Although DPEs, γ-butyrolactones, and CPs have been identified in *Aspergillus* species [3,9–11], significant breakthroughs in the discovery of their hybrids or spiro-diphenyl ethers have yet to be achieved.

As part of our ongoing study on the endophytic fungi associated with *Bufo gargarizans* [19,20], *Aspergillus* sp. F1–8A was isolated from the parotoid gland secretions of *Bufo gargarizans.* Screening of various culture media (Fig. S1 in Supporting information) led to the isolation of five previously undescribed diphenyl ethers hybrids (**1**–**5**) and two spiro-diphenyl ethers (**6**, **7**) (Fig. 1). To the

* Corresponding author.
E-mail address: Lplin@njucm.edu.cn (L.-P. Lin).

https://doi.org/10.1016/j.cclet.2025.111121
1001-8417/© 2025 Published by Elsevier B.V. on behalf of Chinese Chemical Society and Institute of Materia Medica, Chinese Academy of Medical Sciences.

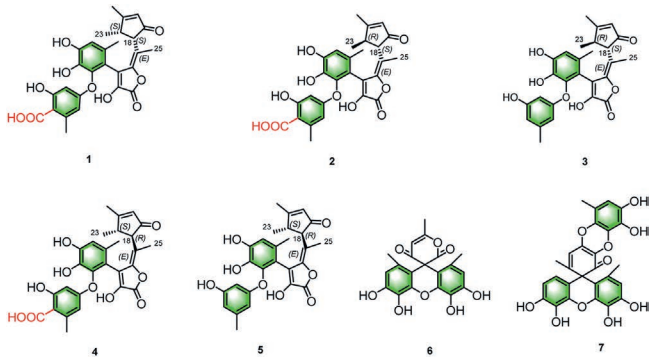


Fig. 1. The structures of compounds **1**–**7**.

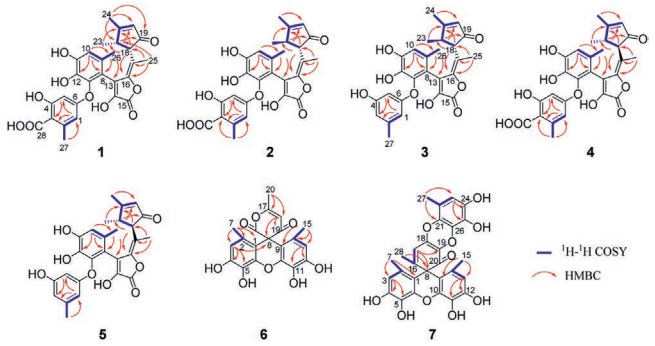


Fig. 2. Key ^{1}H-^{1}H COSY and HMBC correlations of compounds **1**–**7**.

best of our knowledge, asplactones A–E (**1**–**5**) represent the first naturally occurring hybrids composed of diphenyl ethers, conjugated γ-butyrolactones, and CPs. *Aspviolaceol* A (**6**) and B (**7**) are the first known natural spiro-diphenyl ethers. Compounds **1**, **2**, **4**, **6**, and **7** exhibited strong antioxidant activity both *in vitro* and *in vivo*. This report details the isolation, structural characterization, proposed biosynthetic pathways, and antioxidant activities of these novel diphenyl ether derivatives.

Asplactone A (**1**) was isolated as a light yellow powder with a molecular formula of $C_{28}H_{26}O_{10}$, deduced from high-resolution electrospray ionization mass spectrometry (HR-ESI-MS) analysis. The molecular ion peak at *m/z* 523.1594 $[M+H]^+$ (calcd. for $C_{28}H_{27}O_{10}$, 523.1599) indicated 16 degrees of unsaturation, consistent with the carbon-13 nuclear magnetic resonance (^{13}C NMR) data. The infrared (IR) spectrum displayed absorption bands corresponding to hydroxyl (3731 cm^{-1}) and γ-lactone (1744 cm^{-1}) functional groups (Fig. S2 in Supporting information). The ^{1}H NMR (Table S2 in Supporting information) and ^{13}C NMR (Table S3 in Supporting information) spectra displayed characteristic signals for a C-8 substituted gerfelin moiety, including δ_H 6.16 (1H, d, J = 2.5 Hz, H-1), 6.06 (1H, d, J = 2.5 Hz, H-5), 6.68 (1H, s, H-10), 2.04 (3H, s, Me-26), 2.34 (3H, s, Me-27), and δ_C 141.7 (C-2), 108.6 (C-3), 160.9 (C-4), 162.9 (C-6), 142.8 (C-7), 114.6 (C-8), 127.6 (C-9), 147.7 (C-11), 136.2 (C-12), and 172.6 (C-28). Key ^{1}H–^{1}H COSY correlations (Fig. S8 in Supporting information) revealed two independent spin systems [Me-27/H-1 and Me-26/H-10] (Fig. 2). Heteronuclear multiple bond correlation (HMBC) analysis (Fig. S10 in Supporting information) revealed correlations from Me-27 to C-1 and C-2, and from Me-26 to C-10 and C-8, which aided in establishing the planar structure of the diphenyl ether core (rings A and B) (Figs. 1 and 2) [21].

Additional NMR signals included two methyl singlets [δ_H 1.97 (s, 3H, Me-24) and 1.66 (s, 3H, Me-25)], one methyl doublet [δ_H 0.96 (3H, d, J = 7.0 Hz), Me-23], two methine protons [δ_H 2.21 (1H, dq, J = 15.0, 7.0 Hz, H-22) and 3.33 (1H, d, J = 7.0 Hz, H-18)], and

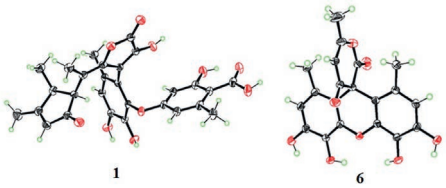


Fig. 3. X-ray crystal structures of **1** and **6**.

an olefinic proton (δ_H 5.88, s, H-20) (Table S2). The ^{13}C NMR data revealed the presence of a ketone carbonyl (δ_C 206.0, C-19), an ester carbonyl (δ_C 163.6, C-15)], six olefinic carbons [δ_C 119.4 (C-13), 139.5 (C-14), 144.7 (C-16), 116.5 (C-17), 129.0 (C-20), and 182.7 (C-21)], and two methine carbons [δ_C 51.0 (C-18) and 43.6 (C-22)] (Table S3). ^{1}H–^{1}H correlation spectroscopy (COSY) correlations indicated an independent spin system connecting H-20, Me-24, H-22, Me-23, and H-18 (Fig. 2). Moreover, HMBC correlations from Me-25 to C-16, C-17, C-18, and C-22; from Me-24 to C-19, C-20, and C-22; from Me-23 to C-18 and C-21; and from H-22 to C-19 and C-20 (Fig. 2), along with the remaining 7 degrees of unsaturation, supported the structural assignment of a conjugated γ-butyrolactone (ring C) and a CP (ring D) moiety. The connectivity of the diphenyl ether core with the conjugated γ-butyrolactone and CP units was further established by HMBC correlations from Me-26 to C-13 and from Me-25 to C-16 and C-18 (Fig. 2).

The *cis*-configuration of H-18 and H-22 was evidenced by nuclear Overhauser effect spectroscopy (NOESY) correlations between H-22 (δ_H 2.21) and H-18 (δ_H 3.33), as well as between Me-25 (δ_H 1.66) and Me-23 (δ_H 0.96) (Figs. S11, S12, and S64 in Supporting information). Finally, the 18*S*, 22*S* configurations of **1**, along with the *E*-geomtry of the $\Delta^{16,17}$ double bond, were unequivocally determined through single-crystal X-ray diffraction (Fig. 3).

Asplactone B (**2**) was isolated as a light yellow powder. Its molecular formula was determined to be $C_{28}H_{26}O_{10}$ based on HR-ESI-MS (*m/z* 545.1411 $[M+Na]^+$, calcd. for $C_{28}H_{26}O_{10}Na$, 545.1418). The IR spectrum indicated the presence of hydroxyl (3731 cm^{-1}) and γ-lactone (1746 cm^{-1}) functional groups (Fig. S15 in Supporting information). High performance liquid chromatography (HPLC) analysis baseline-separated of compounds **1** and **2** were on an RP-18 column (Fig. S2A in Supporting information), with similar ultraviolet (UV) spectra (Figs. S2B and C in Supporting information). Analysis of the 1D (Tables S2 and S3) and 2D NMR (Fig. 2 and Figs. S20–S24 in Supporting information) spectra revealed that the NMR spectra for **2** were similar to those of **1**. However, the upfield shift of H-18 (δ_H 3.03), the downfield shift of H-22 (δ_H 2.66), and H_3–23 (δ_H 1.12) in the ^{1}H NMR (Table S2), as well as upfield chemical shifts of C-23 (compound **1**: δ_C 14.1; compound **2**: δ_C 13.3) in the ^{13}C NMR (Table S3), compared to compound **1** [H-18 (δ_H 3.33), H-22 (δ_H 2.21), and H_3–23 (δ_H 0.96)], along with the opposite specific optical rotation values (**1**: −73.30, **2**: +51.67), suggest that compound **2** is a C-22 epimer of **1** and adopts a 22*R*-configuration. The *trans*-configuration of H-18 and H-22 was further supported by the NOESY correlations (Fig. S23 in Supporting information) between H_3–23 (δ_H 1.12) and H-18 (δ_H 3.03), and between H_3–25 (δ_H 1.60) and H-22 (δ_H 2.66) (Figs. S24 and S64 in Supporting information). The stereochemistry of **2** was ultimately determined to be 18*S*, 22*R* by comparing electronic circular dichroism (ECD) calculations with experimental circular dichroism (CD) data (Fig. 4A and Table S4 in Supporting information).

Asplactone C (**3**) was obtained as a light yellow powder with a molecular formula of $C_{27}H_{26}O_8$, corresponding to 15 degrees of unsaturation and a molecular weight 44 Da less than that of compound **2** (*vide supra*). This was corroborated by its HR-ESI-MS ion at *m/z* 477.1559 $[M-H]^-$ (calcd. for $C_{27}H_{25}O_8$, 477.1555). Analysis of

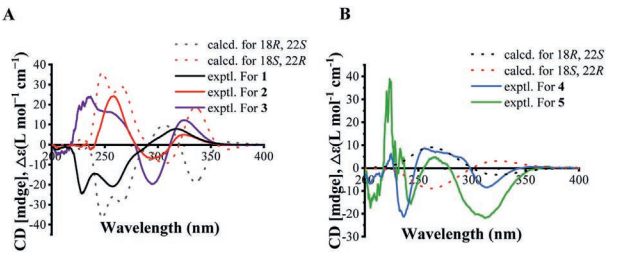


Fig. 4. Stereochemical assignments of compounds **1**–**5** through comparative analysis of experimental CD spectra and computed spectra of potential stereoisomers.

the 1D and 2D NMR data revealed that the structure of **3** closely resembled that of **2**, except for the absence of a carboxyl group (δ_C 172.5), which was further supported by the appearance of an additional proton at H-3 (δ_H 6.00) and the upfield shift of H_3–27 (δ_H 2.09) (Tables S2 and S3). In the HPLC analysis, the retention time of compound **3** was adjacent to that of compounds **1** and **2** (Fig. S2A), with a slightly different UV profile (Fig. S2B). Additionally, the ECD profile of **3** closely matched that of compound **2**, and its stereochemistry was confirmed as 18*S*, 22*R* by comparing ECD calculations with the experimental CD data (Fig. 4A and Table S5 in Supporting information).

By comparing the configurations of compounds **1**–**3** with their corresponding CD spectra, it can be concluded that the positive Cotton effect observed in the 220–280 nm range, coupled with the negative Cotton effect in the 280–310 nm range, suggests the 22*R*-configuration. In contrast, the 22*S*-configuration is implied in the opposite scenario. Additionally, the positive Cotton effect observed in the 310–350 nm range is indicative of the 18*S*-configuration (Fig. 4A).

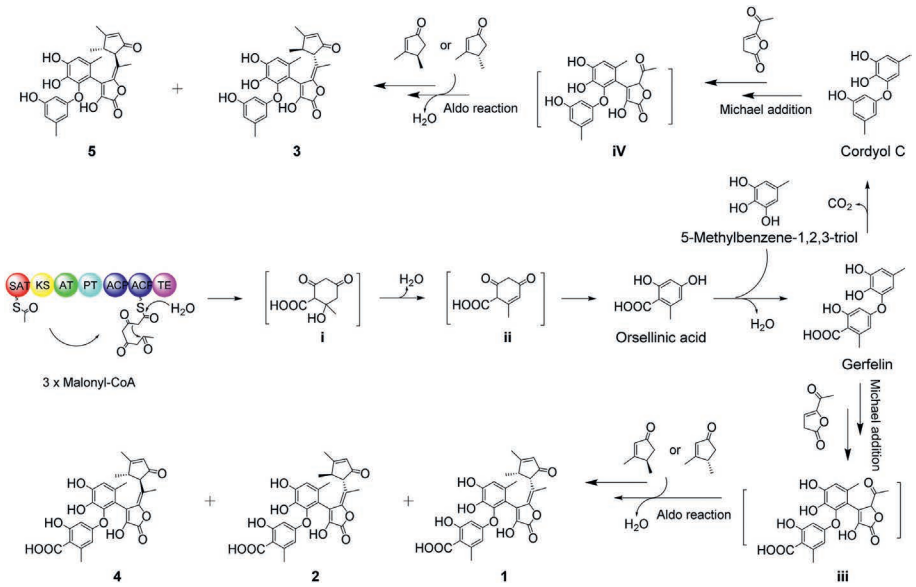
Asplactone D (**4**) was isolated as a light yellow powder, and its molecular formula was determined to be the same as that of compounds **1** and **2**, based on the HR-ESI-MS ions at *m/z* 523.1593 $[M+H]^+$ (calcd. for $C_{28}H_{27}O_{10}$, 523.1599). The IR spectral data (Fig. S39 in Supporting information) and UV profile of **4** (Figs. S2B and C) closely resembled those of compounds **1** and **2**. HPLC analysis over an Eclipse XDB-C18 column indicated that compounds **1**, **2**, and **4** could be baseline-separated (Fig. S2A). However, the slight upfield shift of H-18 (δ_H 3.26) and the significant upfield shift of H_3–25 (δ_H 1.08) in the ^{1}H NMR (Table S2), compared to compound **1** [H-18 (δ_H 3.33) and H_3–25 (δ_H 1.66)], suggest that compound **4** is a C-18 epimer of **1** and likely adopts an 18*R*-configuration. This hypothesis is further supported by the notable downfield shift of C-18 (compound **1**: δ_C 51.0; compound **4**: δ_C 56.7) and the upfield shift of C-25 (compound **1**: δ_C 16.2; compound **4**: δ_C 10.7) in the ^{13}C NMR (Table S3). Additionally, the opposite configuration of **4** compared to **3** was confirmed by the reversed specific optical rotation values (**3**: +20.00, **4**: −28.00). The negative Cotton effect observed around 220–250 nm and 310–350 nm, couple with the positive Cotton effect in the 250–300 nm range, indicates the 22*S*-configuration for compound **4** (Fig. 4B). Ultimately, the 18*R*, 22*S* configuration of **4** was established through ECD calculations for the 18*R*, 22*S* and 18*S*, 22*R* stereoisomers (Fig. 4B). However, compared to compounds **1**–**3**, the geometry of the $\Delta^{16,17}$ double bond in **4** remained uncertain and required further confirmation (Table S3). To address this, the ^{13}C NMR chemical shifts for both the **4***Z* and **4***E* diastereomers of **4** were calculated at the B3LYP/6–31+G (d, p) level in polarizable continuum model (PCM) dimethylsulfoxide. The **4***E* configuration was determined by the 100% DP4+ probability and the excellent correlation coefficient (R^2) between the experimental ^{13}C NMR for **4** and the calculated data for **4***E* diastereomer (Fig. S51 and Tables S6 and S7 in Supporting information).

Asplactone D (**5**) was isolated as a light yellow powder with a molecular formula of $C_{27}H_{26}O_8$ (15 degrees of unsaturation), which is 44 Da less than that of compound **4** (*vide supra*). This was confirmed by its HR-ESI-MS ion at *m/z* 477.1559 $[M-H]^-$ (calcd. for $C_{27}H_{25}O_8$, 477.1555). Comparisons of the 1D and 2D NMR spectra (Tables S2 and S3) suggest that compound **5** is a 3-deacetyl derivative of **4**. This was further supported by the disappearance of the δ_C 172.7 signal (Table S3) and the appearance of an extra proton at H-3 (δ_H 5.94) in **5** (Table S2), as well as a significant upfield shift of Me-27 signal from δ_H 2.37 (s) to 2.08 (s) in comparison to **4**. The absolute configuration of **5** was established as 18*R*, 22*S* by comparing its experimental ECD profiles with those of **4** and with the ECD spectra calculated for 18*R*, 22*S* and 18*S*, 22*R* stereoisomers (Fig. 4B)

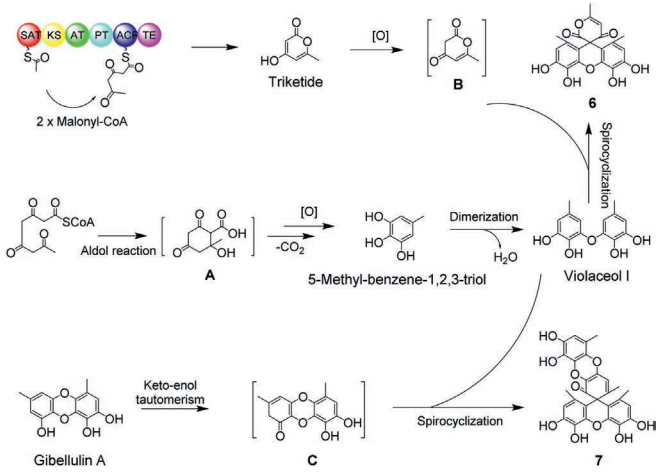
Aspviolaceol A (**6**) was isolated as a yellow powder, with a molecular formula of $C_{20}H_{16}O_8$, determined by HR-ESI-MS at *m/z* 385.0920 $[M+H]^+$ (calcd. for $C_{20}H_{17}O_8$, 385.0918), indicating 13 degrees of unsaturation. The ^{13}C NMR spectrum (Fig. S68 in Supporting information) displayed 13 carbon signals, suggesting partial symmetry in the structure of **6**. Compared to violaceol I [22], the ^{1}H NMR (Fig. S67 in Supporting information) of **6** exhibits an additional methyl signal at δ_H 2.29 (3H, s, H_3–20) and an olefinic proton (δ_H 6.13, s, H-18) (Table S2). Furthermore, the ^{13}C NMR spectrum of **6** showed six extra carbon signals compared to violaceol I, including one ester carbonyl (δ_C 172.5, C-16), one ketone carbonyl (δ_C 194.4, C-19), two olefinic carbons [C-17 (δ_C 170.1) and C-18 (δ_C 109.9)], one sp^3 quaternary carbon (δ_C 58.2, C-8), and one methyl group (δ_C 20.4, C-20) attached to the $\Delta^{17,18}$ double bond (Table S3). A 6-methyl-pyran-2,4-dione structure was proposed based on the HMBC correlations (Fig. S72 in Supporting information) from Me-20 to C-17/C-18 and H-18 to C-8/C-17/C-19/C-20. Moreover, the pyranone moiety was fused with violaceol I through C-8 spirocyclization, as established by the key HMBC correlations of H-18 (δ_H 6.13, s) and H-3 (δ_H 6.40, s) to C-8 (δ_C 58.2) (Fig. 2). The proposed structure for compound **6** was eventually confirmed by single-crystal X-ray diffraction (Fig. 3), and the P-1 space group indicates that **6** is archiral.

Aspviolaceol A (**7**) was obtained as a reddish-brown powder with a molecular formula of $C_{28}H_{22}O_{10}$, indicating 18 degrees of unsaturation, as determined by HR-ESI-MS at *m/z* 517.1156 $[M-H]^-$ (calcd. for $C_{28}H_{21}O_{10}$, 517.1140). Further analysis of the ^{1}H (Fig. S76 in Supporting information) and ^{13}C NMR (Fig. S77 in Supporting information) data revealed that rings A to C in compound **7** closely resembled those of violaceol I [22], while the remaining moiety of **7** closely resembled gibellulin A [23]. However, the C-1 and C-9 positions of the violaceol I moiety in **7** were fused with gibellulin A *via* a C-8 spirocyclization [23], as evidenced by the absence of two aromatic protons at δ_H 6.15 (m) [22], the significant upfield shift of C-8 from δ_C 111.5 to δ_C 59.1, and the absence of a singlet aromatic proton at δ_H 6.33 compared to violaceol I and gibellulin A, respectively [23]. Furthermore, the hydroxy group in gibellulin A was oxidized into a ketone carbonyl, as indicated by the notable downfield shift of C-20 from δ_C 145.0 to δ_C 195.2 in **7**. Finally, the unprecedented heterodimer **7**, constructed *via* a spirocyclization reaction between violaceol I and the oxidized gibellulin A, was confirmed by the four spin-coupling fragments in its ^{1}H-^{1}H COSY spectrum (Fig. 2 and Fig. S79 in Supporting information), along with the HMBC correlations from Me-28 to C-8/C-16/C-17, and from H-17 to C-8/C-19 (Fig. 2).

Interestingly, the metabolites of *Aspergillus* sp. F1–8A, associated with toad venom, are completely different from the chemical components of toad venom itself, suggesting that the presence of the endophytic fungus introduces additional compounds and potential bioactivities to the medicinal material. Biogenetically, the precursor of compounds **1**–**5** originate from malonyl-CoA, which, under the catalysis of polyketide sythase (PKS), is converted to orsellinic acid [24]. This intermediate undergoes dehydration with 5-methyl-benzene-1,2,3-triol to form gerfelin, which is sub-



Scheme 1. Proposed biosynthetic pathway for **1**–**5**.



Scheme 2. Proposed biosynthetic pathway for **6** and **7**.

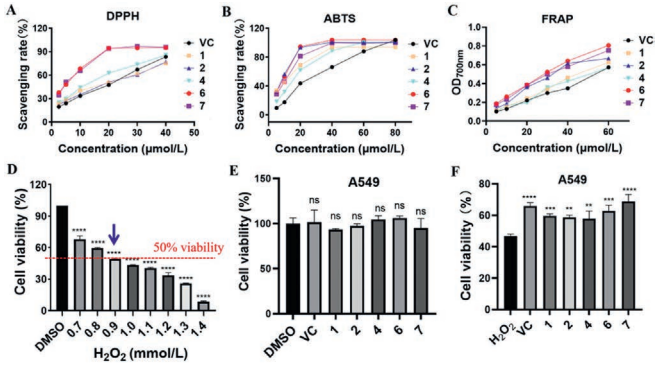


Fig. 5. Antioxidant ability and cytoprotective effects of the tested compounds. DPPH (A) and ABTS (B) free radical scavenging ability, expressed as scavenging rate (%), with VC used as the control. (C) Ferric reducing ability, expressed as optical density (OD) at 700 nm, with VC as the control. (D) Effects of H_2O_2 at various concentrations (0.7, 0.8, 0.9, 1.0, 1.1, 1.2, 1.3, and 1.4 mmol/L) on the viability of A549 cells. (E) Cytotoxicity of the tested compounds and VC (all at 20 μmol/L) on A549 cells, with DMSO as the negative control (ns, no significance). (F) Protective effects of the tested compounds (20 μmol/L) against H_2O_2-induced oxidative damage in A549 cells, with 0.9 mmol/L H_2O_2 treatment as the model group. Results are expressed as mean ± SD ($n = 3$). $^{**}P < 0.01$, $^{***}P < 0.001$, $^{****}P < 0.0001$ *vs.* the DMSO control or the model group.

sequently decarboxylated to yield cordyol C [25]. Both gerfelin and cordyol C can undergo a Michael addition reaction with 5-acetylfuran-2(*3H*)-one, resulting in the formation of intermediates **iii** and **iv**, respectively. These intermediates then undergo aldol reactions with (*S* or *R*)-3,4-dimethylcyclopent-2-en-1-one to produce compounds **1**, **2**, **4** and compounds **3**, **5**, respectively (Scheme 1). For the biosynthesis of spiro-diphenyl ethers **6** and **7**, two 5-methyl-benzene-1,2,3-triol units [26] act as the upstream precursor, undergoing dehydration to form violaceol I [22]. Violaceol I then undergoes spirocyclization with triketone B [24] to yield aspviolaceol A (**6**). Additionally, gibellulin A undergoes keto-enol tautomerism to form intermediate C, which then undergoes spirocyclization with violaceol I to produce aspviolaceol B (**7**) (Scheme 2).

Compounds **1**–**7** were evaluated for their *in vitro* antioxidant ability and cytoprotective effects, with the exception of **3** and **5**, which were not tested due to insufficient quantities. Antioxidant ability was assessed using the 1,1-diphenyl-2-picrylhydrazyl (DPPH) and 2,2′-azino-bis(3-ethylbenzothiazoline-6-sulfonate) (ABTS) radical scavenging assays, and the ferric reducing antioxidant power (FRAP) method [27]. Compounds **1**, **2**, **4**, **6**, and **7** exhibited significant DPPH$^{\bullet}$ (Fig. 5A and Table S8 in Supporting information) and ABTS$^{\bullet+}$ scavenging abilities (Fig. 5B and Table S8), as well as strong ferric reducing power (Fig. 5C), comparable to or exceeding the positive control (ascorbic acid or vitamin C (VC)) (Fig. 5 and Table S8). A549 cells treated with 0.9 mmol/L H_2O_2 showed a viability of 50% ± 0.44% (Fig. 5D), establishing this concentration as suitable for subsequent experiments. Further investigation revealed that pretreatment with compounds **1**, **2**, **4**, **6**, and **7** (all at 20 μmol/L) had no significant effect on A549 cell viability (Fig. 5E), but significantly improved the viability of A549 cells damaged by 0.9 mmol/L H_2O_2, matching or surpassing the effects of vitamin C (Fig. 5F) [28]. These findings suggest that compounds **1**, **2**, **4**, **6**, and **7** exhibit excellent *in vitro* antioxidant ability and cytoprotective effects against H_2O_2-induced cellular damage.

In summary, this study marks the first discovery of asplactones A–E (**1**–**5**), which represent the first examples of diphenyl ethers fused with unusual conjugated γ-butyrolactone and CP moieties, implying that **1**–**5** are representatives of a new subclass within the diphenyl ether family. Furthermore, these are the first documented natural products with a hybrid structure that integrates both CP

and γ-butyrolactone moieties. Additionally, aspviolaceols A (**6**) and B (**7**) represent the only two examples of spiro-diphenyl ethers found in nature to date. This work marks a significant milestone in decades of research on *Aspergillus,* showcasing the remarkable chemical ingenuity of this genus. The discovery of these unique diphenyl ether hybrids and spiro-diphenyl ethers has expanded the structural diversity of the natural product library and their excellent antioxidant properties and cytoprotective effects provide promising insights for further pharmacological investigation.

Declaration of competing interest

The authors declare that they have no known competing financial interests or personal relationships that could have appeared to influence the work reported in this paper.

CRediT authorship contribution statement

Hai-Ying Yu: Writing – original draft, Methodology, Investigation, Data curation. **Yu-Wei Huang:** Methodology, Investigation, Formal analysis, Data curation. **Li-Ping Lin:** Writing – review & editing, Visualization, Validation, Supervision, Resources, Project administration, Methodology, Investigation, Funding acquisition, Formal analysis, Data curation, Conceptualization. **Ren-Xiang Tan:** Supervision, Project administration.

Acknowledgments

This work was financially supported by the National Natural Science Foundation of China (No. 82073721) and Major Basic Research Project of the Natural Science Foundation of the Jiangsu Higher Education Institutions of China (No. 23KJA310003).

Supplementary materials

Supplementary material associated with this article can be found, in the online version, at doi:10.1016/j.cclet.2025.111121.

References

[1] B. Liu, Y.X. Wang, N. Chen, et al., Mini-Rev. Org. Chem. 21 (2024) 590–598.
[2] X. Tang, M. Xie, Y.X. Sun, et al., Chin. Chem. Lett. 20 (2009) 435–438.
[3] Y.B. Ji, W.J. Chen, T.Z. Shan, et al., Chem. Biodivers. 17 (2020) e1900640.
[4] S. Zenitani, S. Tashiro, K. Shindo, et al., J. Antibiot. 56 (2003) 617–621.
[5] Q. Zhang, J.X. Pang, T.Z. Wang, et al., Chin. Chem. Lett. 34 (2023) 108121.
[6] J. Hur, J. Jang, J. Sim, Int. J. Mol. Sci. 22 (2021) 2769.
[7] S.H. Burstein, Prostaglandins Other Lipid Mediat. 148 (2020) 106408.
[8] M. Conti, Anticancer Drugs 17 (2006) 1017–1022.
[9] C. Zhou, Y. Ge, D. Lan, et al., Fitoterapia 176 (2024) 106039.
[10] K.M. Kitzinger, J.S. Johnson, Org. Lett. 25 (2023) 7446–7450.
[11] W.S. Song, H. Qi, S.Y. Zhang, et al., J. Asian Nat. Prod. Res. 24 (2022) 1058–1063.
[12] A.M. Fu, C.M. Chen, Q. Li, et al., Chin. Chem. Lett. 35 (2024) 109100.
[13] H. Zhang, C.P. Li, L.L. Wang, et al., Chin. Chem. Lett. 35 (2024) 109351.
[14] C. Sun, Y. Ha, X. Liu, et al., Molecules 29 (2024) 459.
[15] H. Jangid, S. Garg, P. Kashyap, et al., Front. Microbiol. 15 (2024) 1379602.
[16] K. Xu, C.Li X.L.Yuan, et al., Mar. Drugs 18 (2020) 54.
[17] X. Bai, Y. Sheng, Z. Tang, et al., J. Fungi 9 (2023) 261.
[18] R. Orfali, M.A. Aboseada, N.M. Abdel-Wahab, et al., RSC Adv. 11 (2021) 17116–17150.
[19] J. Guan, P.P. Zhang, X.H. Wang, et al., J. Nat. Prod. 87 (2024) 238–251.
[20] P. Li, Z.J. Zhang, Y.T. Guo, et al., Phytochemistry 222 (2024) 114073.
[21] J.F. Sanchez, Y.M. Chiang, E. Szewczyk, et al., Mol. Biosyst. 6 (2010) 587–593.
[22] L.J. Fremlin, A.M. Piggott, E. Lacey, et al., J. Nat. Prod. 72 (2009) 666–670.
[23] F.Y. Lv, X.M. Li, L.P. Chi, et al., J. Oceanol. Limnol. 38 (2020) 1225–1232.
[24] C. Zaehle, M. Gressler, E. Shelest, et al., Chem. Biol. 21 (2014) 719–731.
[25] T. Bunyapaiboonsri, S. Yoiprommarat, K. Intereya, et al., Chem. Pharm. Bull. 55 (2007) 304–307.
[26] M.L. Nielsen, J.B. Nielsen, C. Rank, et al., FEMS Microbiol. Lett. 321 (2011) 157–166.
[27] I. Gulcin, Arch. Toxicol. 94 (2020) 651–715.
[28] B. Ghodsi-Moghadaml, A. Asoodeh, Int. J. Pept. Res. Ther. 25 (2019) 1065–1074.